Hindawi
Advances in Meteorology
Volume 2018, Article ID 2078057, 8 pages
https://doi.org/10.1155/2018/2078057

Research Article

Multiresolution Analysis of the Relationship of Solar Activity, Global Temperatures, and Global Warming

Zhen Li, Jianping Yue, Yunfei Xiang, Jian Chen, Yankai Bian, and Hanqing Chen

School of Earth Sciences and Engineering , Hohai University, Nanjing 211100, China

Correspondence should be addressed to Zhen Li; lizhenhhu@126.com

Received 27 March 2018; Revised 14 May 2018; Accepted 5 June 2018; Published 24 July 2018

Academic Editor: Herminia García Mozo

Sunspot number is an important parameter for presenting the intensity of solar activity. Based on the sunspot number series, which has been replaced by a new improved version since 2015, we confirm that the sunspot number has significant variations at 11-year and 112-year periods. The sunspot number has also increased from 1700 to 2016 with 0.08 annual increments on the basis of wavelet analysis and least-square fitting. We further confirm that global temperatures are remarkable in 22-year and 64-year cycles. The result of wavelet transform coherence (WTC) analysis suggests that solar activity has a positive lag effect on global temperatures in the period band of 22 years with a 3-year lag. However, the linearly increasing global temperature has hampered WTC analysis since 1960. Aiming to solve this problem, we apply wavelet decomposition and cross correlation to determine whether the aforementioned lag effect in the period band of 22 years has a 2-year lag rather than a 3-year lag. We find that the 22-year magnetic field solar cycle plays a greater role in global climate change than the 11-year sunspot cycle. In addition, we notice that the solar activity is not a representation of the driving force of the upward trend of global temperature after the industrial age. The Granger causality test results demonstrate that the phenomenon of the global warming is caused by excessive CO_2 emissions.

1. Introduction

An increase in global temperature in the last 50 years has been observed and is thus considerably discussed [1–3]. A growing number of studies suggest that the increase in greenhouse gas concentrations in the air caused by anthropogenic effects is responsible for the climatic warming [4–6]. The prevailing view of the Intergovernmental Panel on Climate Change (IPCC) suggests that more than 90% of the causes of the significant increase in earth's average temperature over the past 50 years can be attributed to greenhouse gases emitted by human activities, and thus, the impact of climate change can be ignored [7–10]. However, a body of evidence also suggests that solar activity may account for a substantial amount of global temperature variability [11–17]. Eddy [18] proposed the existence of the "Little Ice Age" and the "Medieval Climatic Optimum," which incidentally coincide with Maunder's solar minimum and the grand solar maximum, respectively. Ice core data on several centuries of climate change show that the current global warming belongs to the scope of climate fluctuations [19]. Therefore, the effect of solar activity on the current climate variability cannot be neglected. Valev [20] applied statistical analysis to investigate the correlation between global surface air temperatures and sunspots. However, the method was performed in the time domain rather than the time-frequency space, in which the correlation of some frequency components of two signals can be examined. By using yearly data, Souza Echer et al. [21] performed wavelet multiscale analysis to decompose the sunspot and global temperature time series into five levels and examine their correlation in five different frequency bands. However, their study was limited by the lack of cross validation of higher-resolution data, such as monthly data. Moreover, on July 1, 2015, the sunspot number series was replaced by a new improved version (version 2.0) to include several corrections of past inhomogeneities in the time series. Thus, revisiting the basis of investigating the effects of solar activity and human activity on global climate change is necessary.

In this study, we employ wavelet analysis to detect the period in the sunspot number time series and the global air surface temperature time series by using yearly and monthly

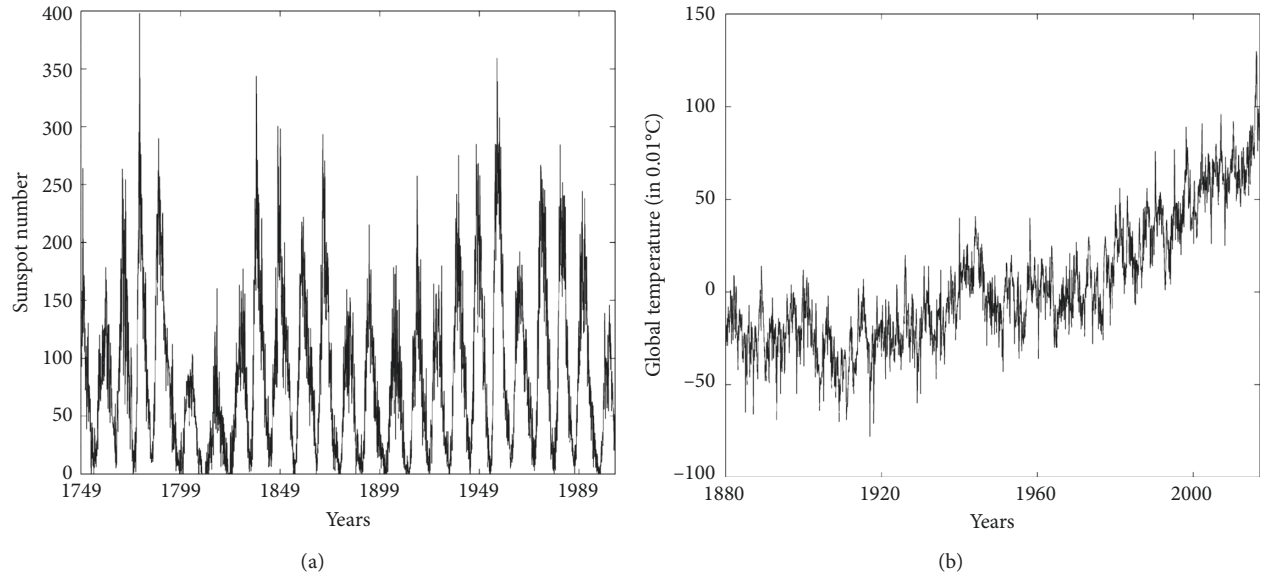

Figure 1: (a) Monthly average of the sunspot number and (b) global surface temperature time-series profiles.

data. Then, based on the monthly data, wavelet transform coherence (WTC) analysis is conducted to investigate the correlation between the two time-series profiles in the time-frequency space. The most significant frequencies for the sunspot number and the global temperature are determined and intercorrelated. Furthermore, wavelet decomposition and the Granger causality test are used to analyze whether global warming is caused by solar activity.

2. Datasets and Methods

2.1. Datasets. For sunspot numbers, we apply the data provided by the Solar Influences Data Analysis Center (http://www.sidc.be/sunspot-data). The data, which are presented by monthly frequencies, cover the period from January 1749 to December 2016. The sunspot number series has been replaced by a new improved set (version 2.0) since 2015. The new time series contains some appreciable improvements, including (i) the adoption of a new reference observer A. Wolfer (a pilot observer from 1876 to 1928) instead of R. Wolf himself and (ii) corrections of several past inhomogeneities in the solar series (Locarno drift correction (1981–2015), Waldmeier jump (1947–1980), Schwabe–Wolf correction (1849–1863), etc.). The details of the new sunspot number series are given by Clette and Lefevre [22] and are not reported here. Meanwhile, the global temperature time-series profiles are obtained from the Goddard Institute for Space Studies surface temperature analysis (GISTEMP) (http://data.giss.nasa.gov/gistemp). The GISTEMP analysis provides a measure of the changing global surface temperature with monthly resolution for the period since 1880, when a reasonably global distribution of meteorological stations was established. The input data that the GISTEMP team uses for the analysis, collected by many national meteorological services around the world, are the adjusted data of the Global Historical Climatology Network (GHCN) version 3, United States Historical Climatology Network (USHCN) data, and SCAR (Scientific Committee on Antarctic Research) data from Antarctic stations. The time-series profiles used in the present study represent monthly deviations in relation to the 1951–1980 average with a scale of 0.01°C and cover the time interval between January 1880 and December 2016.

As shown in Figure 1(a), the sunspot numbers clearly have significant cyclical patterns with time-varying amplitudes, and they exhibit a dominant period every 128 months (approximately 11 years). Meanwhile, as shown in Figure 1(b), the global temperature variabilities are somewhat steady before 1960. However, from 1960 until the end of the analyzed period, a clear upward trend is observed. The upward trend is usually associated with excessive greenhouse gas emissions.

2.2. Methodology of Analysis. The method used in this study includes the analysis of wavelets, including wavelet coherence and wavelet transform. The continuous wavelet transform (CWT) of a time series X_n $(n = 1, 2, \ldots, N)$ is defined [23–25] as

$$W_n^X(s) = \sqrt{\frac{\delta t}{s}} \sum_{n'=1}^{N} X_{n'} \phi_0 \left[(n' - n) \frac{\delta t}{s} \right], \tag{1}$$

where s is the wavelet scale, δt is the time step, ϕ_0 is the mother function, n' is the reversed time, and $\sqrt{\delta t / s}$ is the normalization factor. Compared with traditional methods (e.g., Fourier analysis) that examine continuous and stationary periodic signals in the frequency space, CWT can detect intermittent and/or nonstationary periodicities in the time-frequency space.

After the introduction of CWT, we briefly recall the content of the wavelet coherence to establish our problem context. The wavelet coherence of the two time-series profiles X_n and Y_n $(n = 1, 2, \ldots, N)$ is defined [24–26] as

Table 1: Frequencies corresponding to the scales of the Meyer wavelet function with a 1-year sampling period.

Level	n	Period (years)	Range (years)
D1	1	2	2–4
D2	2	4	4–8
D3	3	8	8–16
D4	4	16	16–32
D5	5	32	32–64
A5	6	64	>64

$$R_n^2(s) = \frac{\left|S\left(s^{-1}W_n^{XY}(s)\right)\right|^2}{S\left(s^{-1}\left|W_n^X(s)\right|^2\right) \cdot S\left(s^{-1}\left|W_n^Y(s)\right|^2\right)}, \quad (2)$$

where S is the smoothing operator, s is the wavelet scale, and $R_n(s)$ is the localized correlation coefficient. For the two CWTs, the WTC can be considered the local correlation between the two time-series profiles in the time-frequency domain. The details of the WTC analysis are given by Grinsted et al. [26] and are not reported here.

The original time series of the sunspot number and the global temperature are the wavelets transformed by the orthonormal discrete Meyer wavelet transform, which decomposes the original signal into orthogonal frequency levels and enables the operation of band-pass filtering in different frequencies, each limited by the power of 2. Wavelet decomposition represents the annual time series of the sunspot number and the global temperature until the D5 level. The corresponding band frequencies are presented in Table 1. The approximations for A5 are at the scaling level and correspond to long-term periods.

3. Results and Discussion

3.1. Period Analysis. Considering that generating the sunspot number variation is a highly complicated nonlinear process, we select here two groups of data to comprehensively analyze the periodicity of sunspot variations. One group is for the monthly sunspot data from 1747 to 2016, while the other group is for the yearly sunspot data from 1700 to 2016. In this analysis, we choose a complex Morlet wavelet with $w_0 = 6$ as the mother function. This value of w_0 offers a good balance between time and frequency localization.

Figure 2 shows the first, second, and third periods located in the period bands of 8–16, 64–128, and 16–32 years, respectively. The 11-year cycle that corresponds to the 8- to 16-year scale has passed the significance test at the 5% level against the red-noise variance test. However, the 112-year cycle for the 64- to 128-year scale and the 22-year cycle for the 16- to 32-year scale are not significant at the same test conditions. The result in Figure 2 indicates that the sunspot in 11-year cycles is significant in the entire time domain, while the 22-year and 112-year cycles are remarkable in the local time domain. In addition, we find that the intensity of the solar activity in the latter half of the twentieth century has reached the highest level since 1749, but the intensity significantly weakened since the twenty-first century.

Figure 3 shows the first, second, and third periods located in the period bands of 8–16, 64–128, and 32–64 years, respectively. The 11-year period corresponding to the 8- to 16-year scale has passed the significance test. However, the 55-year period for the 32- to 64-year scale and the 112-year period for the 64- to 128-year scale have not passed the red-noise test, which indicates that the sunspot number variability is globally significant in 11-year periods and locally notable in 55-year and 112-year periods.

The results of Figures 2 and 3 indicate that the selected different time intervals and timescales correspond to different periods, which is consistent with previous results [27–30]. Moreover, the sunspot number variability is globally significant in 11-year and 112-year cycles and locally remarkable in 22-year and 55-year periods. On the basis of the yearly sunspot numbers from 1700 to 2016 and the sunspot variability cycles determined by the wavelet analysis, this study adopts 11, 22, 55, and 112 years as the period terms of the time-curve fitting equation. The least-square method is used to calculate the amplitude, phase, and trend of the sunspot time series. The curve fitting equation is

$$y = a_0 + a_1 t + a_2 t^2 + \sum_{i=1}^{n} b_i \sin\left(\frac{2\pi t}{T} + \phi\right), \quad (3)$$

where a_0 is the constant, a_1 is the linear trend, a_2 is the linear acceleration, b_i is the amplitude, and T is the period.

Table 2 shows the amplitude of each period and the linear trend of sunspot number variability. The result of Table 2 indicates that the amplitude of 11 years is the maximum and the amplitude of 22 years is the minimum. The sunspot number shows an increasing trend from 1700 to 2016 with 0.08 annual increments, and we can see that the new sunspot number displays a weak trend, which is consistent with the findings of Clette and Lefevre [22].

Moreover, we compare the original values of the sunspot number with the fitting ones. It is clear from Figure 4 that although errors have been observed between original data and fitting data, this fitting scheme describes well the general behavior of solar activity. Meanwhile, the wavelet analysis of the monthly global temperature data from 1880 to 2016 is completed.

Figure 5 shows the first, second, and third periods of global surface temperature variation located in the period bands of 64–128, 16–32, and 8–16 years, respectively. The 64-year period corresponding to the 64- to 128-year scale has passed the significance test, consistent with previous results [31, 32]. The 22-year period corresponding to the 16- to 32-year scale has also passed the significance test, consistent with previous results [33, 34]. However, the 11-year period for the 8- to 16-year scale has not passed the red-noise test, which means that the global surface temperature variation is globally significant in 64-year and 22-year periods and locally notable in 11-year periods.

3.2. Wavelet Coherence Analysis. Considering that the traditional correlation analysis can be performed in the time domain only, we use WTC to find regions in the time-frequency domain where the sunspot time series and the

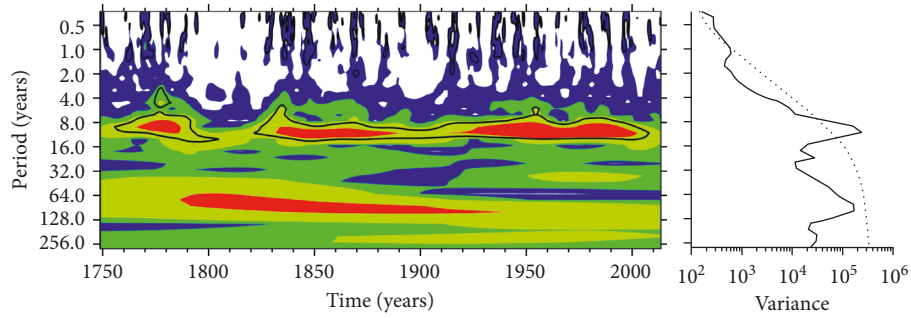

Figure 2: Wavelet power spectrum of monthly sunspots from 1749 to 2016.

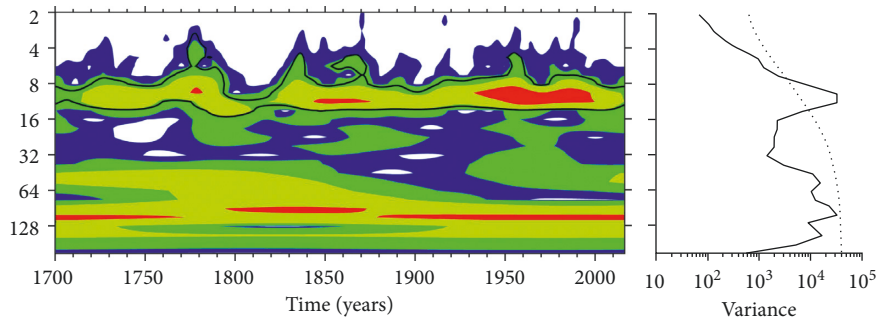

Figure 3: Wavelet power spectrum of the annual sunspots from 1700 to 2016.

Table 2: Parameters of significant periods of the sunspot number time series.

Period	Amplitude	Linear trend
11	47.4	0.08
22	6.7	
55	13.2	
112	22.8	

global temperature time series are highly correlated but do not necessarily have high power values (Figure 6).

The thick contour represents the 5% significance level against red noise, and it is the boundary line of the cone influence in which wavelet power caused by discontinuity at the edge has dropped to e^{-2} of the edge value. The relative phasing relationship is shown as arrows (i.e., in-phase to the right, antiphase to the left, and sunspot number variability leading to global temperature variation of 90° downward). As shown in Figure 6, the most prominent regions with significant correlations are the period scales every 256 months (approximately 22 years), and the correlation in the 11-year period band is low, which is consistent with previous research results [20, 21]. The arrows that point southeastward represent the sunspot number variability that leads to global temperature variation, and the fluctuation range of the time-varying relative phase angle is not large in the 256-month scale. Thus, we adopt the average value of the time-varying relative phase angle to express the phase relationship between the sunspot number and the global temperature. The mean relative phase angle is 50.1°, which is equivalent to

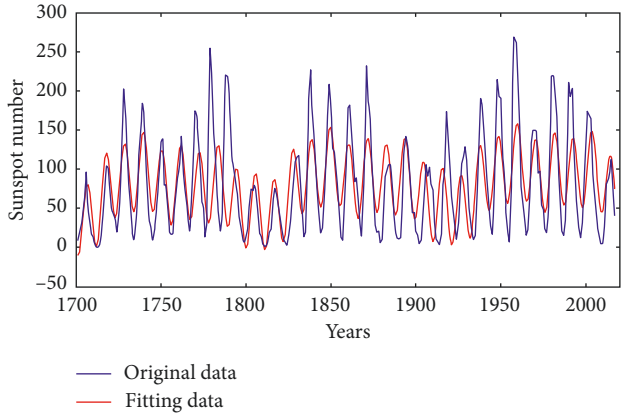

Figure 4: A comparison of the original values of the sunspot number with the fitting ones.

a 3-year lag. However, when the global temperature has started to increase in the 1960s, the high correlation between the sunspot number and the global temperature diminished. This phenomenon indicates that the linearly increasing global temperature will hamper the WTC. Therefore, we use wavelet decomposition to gain deep insights into the correlation between the sunspot and global temperature, and we investigate in more detail the levels D3 (8–16 years), D4 (16–32 years), and A5 (>64 years).

The levels encompass 11-year, 22-year, and long-term trends. Figure 7 presents the D3, D4, and A5 decomposition levels of the sunspot number and global temperature.

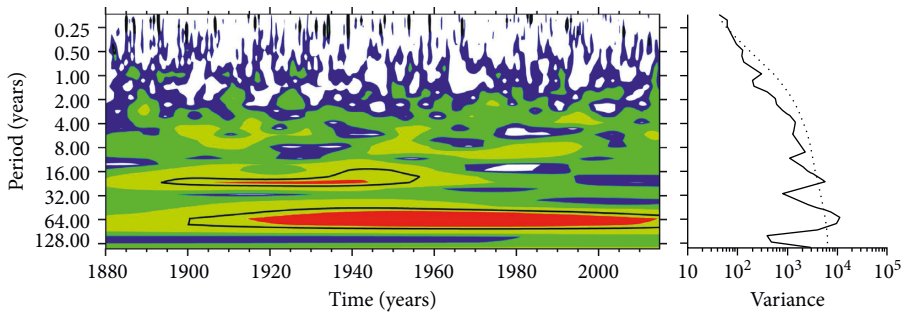

Figure 5: Wavelet power spectrum of monthly global temperatures from 1880 to 2016.

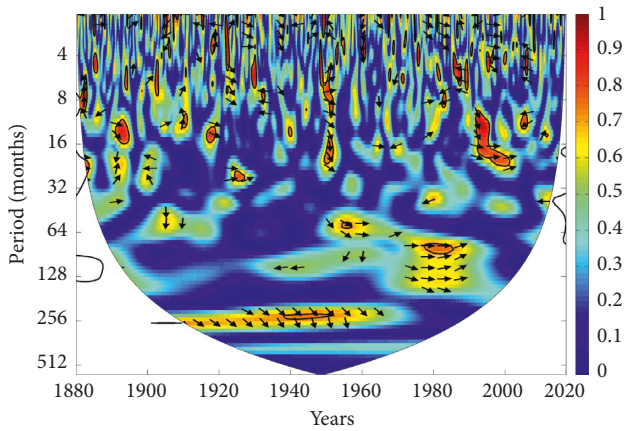

Figure 6: Wavelet coherence spectrum of monthly sunspots and monthly global temperatures.

As shown in Figure 7(a), the 11-year signal in the sunspot time series is the antiphase of the global temperature time series for most of the time periods (i.e., before 1960 and after 2000), while the two signals are in-phase only in 1960–2000. In addition, the distorted waveforms for 1920–1940 and 1950–1970 may explain why only the locally notable 11-year cycle of the global temperature is detected by CWT. As shown in Figure 7(b), the 22-year signal in the two series datasets is in the in-phase before 1920 and after 1990, and sunspot variations always result in global temperature changes for most time periods (i.e., 1920–1990). Meanwhile, we find that the D3 level of GISS temperature calculated by Souza Echer et al. [21] showed a weak 11-year cycle over 1925–1960; however, the 11-year periodical variation is quite normal in this study, which may be attributed to the difference between GHCN version 3 (this represents a change from the prior use of unadjusted version 2 data) and GHCN version 2. Moreover, the cross correlation is taken as an indicator to individually evaluate the performances of different spectral bands [35, 36]. As shown in Figure 8, the cross correlation between the sunspot and global temperature in the D3 band is low and ranges from −0.24 to 0.18. The cross correlation between the two time-series profiles in the D4 band shows significant correlation coefficients with values from −0.6 to 0.59, in which the maximum is 0.59 with a 2-year lag rather than a 3-year lag, which is not consistent with the wavelet-coherent result in Figure 6. The results in Figure 8 indicate that the effect of the 22-year solar cycle is more significant on global temperature than the 11-year cycle, and the linearly increasing global temperature has indeed hampered the WTC. In general, the 22-year period of the solar activity, which is called the magnetic Hale cycle, is related to the change in the sun's magnetic field polarity. Thus, the 22-year magnetic field solar cycle plays a greater role than the 11-year sunspot cycle in global climate change. The approximation level (A5) shows the long-term trends. After 1970, the trend is observed in the opposite direction (Figure 7), which indicates that solar activity does not represent the driving force of the upward trend in global temperature (i.e., the attribution is mainly to the increase in greenhouse gases).

Considering that global warming is usually attributed to the rising concentrations of carbon dioxide (CO_2), establishing the possible connection is also necessary.

Figure 9 presents the annual emissions of CO_2 from 1880 to 2014 provided by the Carbon Dioxide Information Analysis Center database (http://cdiac.ornal.gov/trends/emis/tre-glob.html). The CO_2 emissions have slowly increased before 1950. After 1950, a sharp growing trend is observed, and this phenomenon may hamper the period correlation detection between the sunspot and global temperature.

To further detect the relationship of sunspots, CO_2 emissions, and global temperatures, we employ the Granger causality test to investigate their dependence on one another [37, 38].

Lag length selection is conducted by using the Bayesian information criterion. A p value >0.1 indicates that there is no Granger causality between the two time-series profiles. The results in Table 3 suggest that global warming is mainly caused by CO_2 emissions rather than sunspot number variability.

4. Conclusion

The results of the wavelet analysis in this study indicate that the sunspot number variability is globally significant in 11-year and 112-year periods and locally remarkable in 22-year and 55-year cycles, while global temperatures are globally notable in 22-year and 64-year cycles and locally remarkable in 11-year periods. Meanwhile, the least-square curve fitting indicates that the amplitude of 11 years is the maximum and the amplitude of 22 years is the minimum. The sunspot number has increased from 1700 to 2016 with 0.08 annual

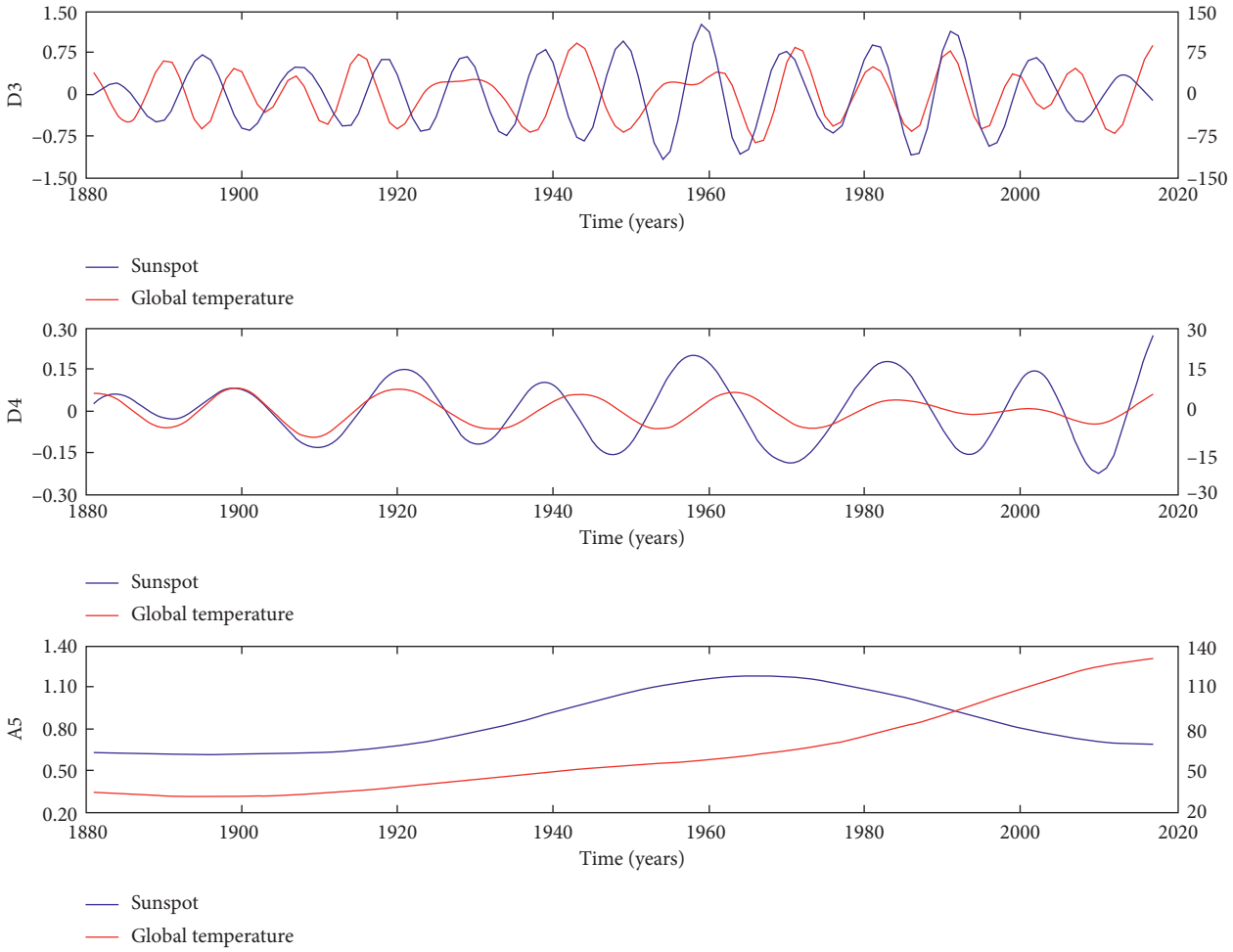

Figure 7: D3 (a), D4 (b), and A5 (c) decomposition levels of the sunspot number and global temperature.

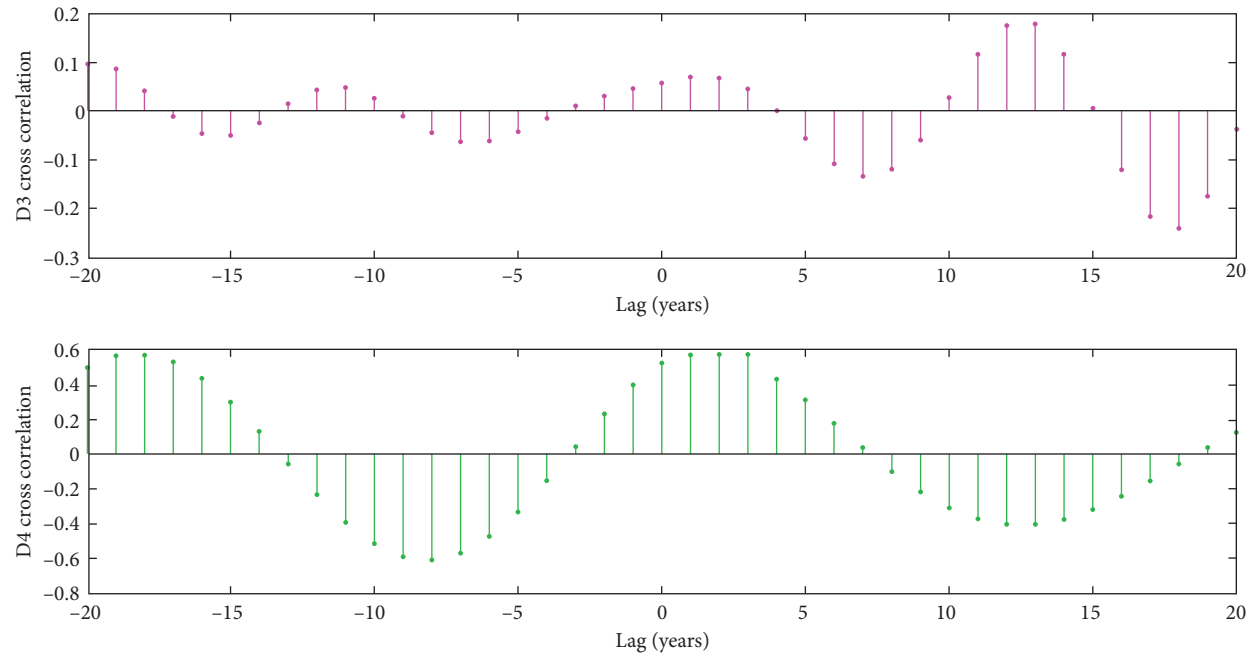

Figure 8: Cross correlation between the sunspot number and global temperature with different lags.

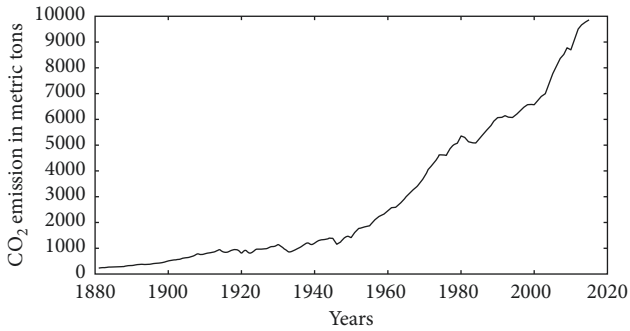

Figure 9: Annual values of carbon dioxide emissions from 1880 to 2014.

Table 3: Granger causality test.

	p value	Lags
Sunspots → global T	0.4	3
CO_2 emissions → global T	$1.4e^{-7}$	3

increments. Furthermore, we apply WTC to confirm whether the solar activity before 1960 has a positive lag effect on global temperatures in the 22-year period band with a 3-year lag. The linearly increasing global temperature has hampered WTC. Then, wavelet decomposition is used to gain deeper insights into the correlation between the sunspot and global temperature. The cross correlation indicates that the effect of the 22-year solar cycle with a 2-year lag on global temperature is more significant than that of the 11-year cycle. Thus, the 22-year magnetic field solar cycle plays a greater role than the 11-year sunspot cycle in global climate change. Additionally, we notice that solar activity cannot explain the upward trend of global temperatures after 1970. Finally, the result of the Granger causality test demonstrates that global warming is mainly caused by CO_2 emissions.

Data Availability

The data used to support the findings of this study are available from the corresponding author upon request.

Conflicts of Interest

The authors declare that they have no conflicts of interest.

Acknowledgments

The authors are very grateful to the Solar Influences Data Analysis Center for providing sunspot data and the Goddard Institute for Space Studies of National Aeronautics and Space Administration for providing global surface temperature data.

References

[1] B. Pittock, "Possible sun–weather correlation," *Nature*, vol. 280, no. 5719, pp. 254-255, 1979.

[2] B. Pittock, "Solar variability, weather and climate: an update," *Quarterly Journal of the Royal Meteorological Society*, vol. 109, no. 459, pp. 23–55, 1983.

[3] H. van Loon and K. Labitzke, "The influence of the 11-year solar cycle on the stratosphere below 30 km: a review," *Space Science Reviews*, vol. 94, no. 1-2, pp. 259–278, 2000.

[4] D. E. Parker, P. D. Jones, A. Bevan, and C. K. Folland, "Interdecadal changes of surface temperature since the late 19th century," *Journal of Geophysical Research*, vol. 99, no. D7, article 14373, 1994.

[5] P. D. Jones, M. New, D. E. Parker, S. Martin, and I. C. Rigor, "Surface air temperature and its changes over the past 150 years," *Reviews of Geophysics*, vol. 37, no. 2, pp. 173–199, 1999.

[6] T. P. Barnett, D. W. Pierce, and R. Schnur, "Detection of anthropogenic climate change in the world's oceans," *Science*, vol. 292, no. 5515, pp. 270–274, 2001.

[7] S. Levitus, J. I. Antonov, J. Wang et al., "Anthropogenic warming of Earth's climate system," *Science*, vol. 292, no. 5515, pp. 267–270, 2001.

[8] Intergovernmental Panel on Climate Change, *Climate Change 2001*, J. T. Houghton, Ed., Cambridge University Press, New York, NY, USA, 2007.

[9] S. Solomon, *Climate Change 2007: The Physical Science Basis–Contribution of Working Group I to the Fourth Assessment Report of the Intergovernmental Panel on Climate Change*, Cambridge University Press, Cambridge, UK, 2007.

[10] D. A. Stone, M. R. Allen, and P. A. Stott, "A multimodel update on the detection and attribution of global surface warming," *Journal of Climate*, vol. 20, no. 3, pp. 517–530, 2007.

[11] E. Friis-Christensen and K. Lassen, "Length of the solar cycle: an indicator of solar activity closely associated with climate," *Science*, vol. 254, no. 5032, pp. 698–700, 1991.

[12] J. Lean, F. Beer, and R. Bradley, "Reconstruction of solar irradiance since 1610: implications for climate change," *Geophysical Research Letters*, vol. 22, no. 23, pp. 3195–3198, 1995.

[13] J. D. Haigh, "The impact of solar variability on climate," *Science*, vol. 272, no. 5264, pp. 981–985, 1996.

[14] J. D. Haigh, "The Sun and the Earth's climate," *Living Reviews in Solar Physics*, vol. 4, 2007.

[15] H. Svensmark, "Cosmoclimatology: a new theory emerges," *Astronomy & Geophysics*, vol. 48, no. 1, pp. 118–124, 2007.

[16] N. Scafetta and B. J. West, "Is climate sensitive to solar variability?," *Physics Today*, vol. 61, no. 3, pp. 50-51, 2008.

[17] F. Gervais, "Anthropogenic CO_2 warming challenged by 60-year cycle," *Earth-Science Reviews*, vol. 155, pp. 129–135, 2016.

[18] J. A. Eddy, "The Maunder minimum," *Science*, vol. 192, no. 4245, pp. 1189–1202, 1976.

[19] W. Dansgaard, S. J. Johnsen, J. Moiler et al., "One thousand centuries of climatic record from Camp Century on the Greenland ice sheet," *Science*, vol. 116, no. 3903, pp. 377–380, 1969.

[20] D. Valev, "Statistical relationships between the surface air temperature anomalies and the solar and geomagnetic activity indices," *Physics and Chemistry of the Earth*, vol. 31, no. 1–3, pp. 109–112, 2006.

[21] M. P. Souza Echer, E. Echer, N. R. Rigozo et al., "On the relationship between global, hemispheric and latitudinal averaged air surface temperature (GISS time series) and solar activity," *Journal of Atmospheric and Solar-Terrestrial Physics*, vol. 74, pp. 87–93, 2012.

[22] F. Clette and L. Lefevre, "The new sunspot number: assembling all corrections," *Solar Physics*, vol. 291, no. 9-10, pp. 2629–2651, 2016.

[23] C. Torrence and G. P. Compo, "A practical guide to wavelet analysis," *Bulletin of the American Meteorological Society*, vol. 79, no. 1, pp. 61–78, 1998.
[24] Z. Li, J. P. Yue, W. Li, D. K. Lu, and X. G Li, "A comparison of hydrological deformation using GPS and global hydrological model for the Eurasian plate," *Advances in Space Research*, vol. 60, no. 3, pp. 587–596, 2017.
[25] Z. Li, J. P. Yue, W. Li, and D Lu, "Investigating mass loading contributes of annual GPS observations for the Eurasian plate," *Journal of Geodynamics*, vol. 111, pp. 43–49, 2017.
[26] A. Grinsted, J. C. Moore, and S. Jevrejeva, "Application of the cross wavelet transform and wavelet coherence to geophysical time series," *Nonlinear Processes Geophysics*, vol. 11, no. 5-6, pp. 561–566, 2004.
[27] J. R. Herman and R. A. Goldberg, *Sun, Weather and Climate*, Scientific and Technical Information Branch, National Aeronautics and Space Administration, Washington, DC, USA, 1978.
[28] D. V. Hoyt and K. H. Schatten, *The Role of the Sun in Climate Change*, Oxford University Press, Oxford, UK, 1997.
[29] R. P. Kane, "Prediction of the sunspot maximum of solar cycle 23 by extrapolation of spectral components," *Solar Physics*, vol. 189, no. 1, pp. 217–224, 1999.
[30] M. G. Ogurtsov, Y. A. Nagovitsyn, G. E. Kocharov et al., "Long-period cycles of the sun's activity recorded in direct solar data and proxies," *Solar Physics*, vol. 211, no. 1-2, pp. 371–394, 2002.
[31] R. P. Kane and N. R. Teixeira, "Power spectrum analysis of the time-series of annual mean surface air temperatures," *Climate Change*, vol. 17, no. 1, pp. 121–130, 1990.
[32] M. E. Schlesinger and N. Ramankutty, "An oscillation in the global climate system of period 65–70 years," *Nature*, vol. 367, no. 6465, pp. 723–726, 1994.
[33] M. Ghil and R. Vautard, "Interdecadal oscillations and the warming trend in global temperature time series," *Nature*, vol. 350, no. 6316, pp. 324–327, 1991.
[34] C. D. Keeling and T. P. Whorf, "Possible forcing of global temperature by the oceanic tides," *Proceedings of the National Academy of Sciences*, vol. 94, no. 16, pp. 8321–8328, 1997.
[35] M. Ozger, A. K. Mishra, and V. P Singh, "Low frequency drought variability associated with climate indices," *Journal of Hydrology*, vol. 364, no. 1-2, pp. 152–162, 2009.
[36] M. Ozger, A. K. Mishra, and V. P. Singh, "Estimating Palmer Drought Severity Index using a wavelet fuzzy logic model based on meteorological variables," *International Journal of Climatology*, vol. 31, no. 13, pp. 2021–2032, 2011.
[37] C. W. J. Granger, "Investigating causal relations by econometrics models and cross-spectral methods," *Econometrica*, vol. 37, no. 3, pp. 424–438, 1969.
[38] C. Magazzino, "The relationship between CO_2 emissions and energy consumption and economic growth in Italy," *International Journal of Sustainable Energy*, vol. 35, no. 9, pp. 844–857, 2016.